Colloids and Surfaces B: Biointerfaces 92 (2012) 327–333

Contents lists available at SciVerse ScienceDirect

Colloids and Surfaces B: Biointerfaces

journal homepage: www.elsevier.com/locate/colsurfb

The interfacial interactions of Tb-doped silica nanoparticles with surfactants and phospholipids revealed through the fluorescent response

Olga D. Bochkova[a], Asiya R. Mustafina[a,*], Alsu R. Mukhametshina[b], Vladimir A. Burilov[b], Viktoriya V. Skripacheva[a], Lucia Ya. Zakharova[a], Svetlana V. Fedorenko[a], Alexander I. Konovalov[a], Svetlana E. Soloveva[a], Igor S. Antipin[b]

[a] A.E. Arbuzov Institute of Organic and Physical Chemistry, Arbuzov Street, 8, 420088, Kazan, Russia
[b] Kazan (Volga Region) Federal University, Kremlevskaya str. 18, 420008, Kazan, Russia

ARTICLE INFO

Article history:
Received 30 September 2011
Received in revised form
17 November 2011
Accepted 8 December 2011
Available online 21 December 2011

Keywords:
Silica nanoparticles
Stimuli responsive colloids
Luminescence
Tb(III) complex

ABSTRACT

The quenching effect of dyes (phenol red and bromothymol blue) on Tb(III)-centered luminescence enables to sense the aggregation of cationic and anionic surfactants near the silica surface of Tb-doped silica nanoparticles (SN) in aqueous solutions. The Tb-centered luminescence of non-decorated SNs is diminished by the inner filter effect of both dyes. The decoration of the silica surface by cationic surfactants induces the quenching through the energy transfer between silica coated Tb(III) complexes and dye anions inserted into surfactant aggregates. Thus the distribution of surfactants aggregates at the silica/water interface and in the bulk of solution greatly affects dynamic quenching efficiency. The displacement of dye anions from the interfacial surfactant adlayer by anionic surfactants and phospholipids is accompanied by the "off–on" switching of Tb(III)-centered luminescence.

© 2011 Elsevier B.V. All rights reserved.

1. Introduction

Fluorescent silica nanoparticles have gained a great attention during recent decades due to their bioanalytical application [1–4]. The correlation between luminescence of nanoparticles and the interfacial interactions is a top of current interest, since nanoparticles for biomarking should exhibit stable in time luminescence, which is not quenched at a binding with biotarget, while stimuli responsive luminescent nanoparticles are required for biosensing [5–13]. Lanthanide centered luminescence is of particular importance for bioanalytical and medical applications [14,15]. Thus lanthanide complexes both in the molecular form and silica coated are widely applied in bioanalysis [16–23]. The sensing of substrates is based on various mechanisms of quenching or enhancement of lanthanide centered luminescence. The energy transfer or so-called Förster mechanism is especially important for silica coated lanthanide based luminophores, since it is significant at rather long distances between luminescent and quenching molecules (1–7 nm) [24,25]. Thus the energy transfer from donors (Eu(III) chelates incorporated into nanoparticles) and proteins labeled with dyes has been successfully applied in the sensing of proteins or their aggregation [26]. The labeling of substrates by dyes is the prerequisite step of the abovementioned route of the fluorescent recognition. The present report introduces novel approach to sense nonlabeled substrates through the fluorescent response of lanthanide doped silica nanoparticles (SNs) with the use of dye molecules as a probe. The applicability of this approach is exemplified in the interfacial interactions of SNs with cationic, as well as anionic surfactants and phospholipids. It is worth noting that the development of the procedure, which can selectively probe the aggregation of surfactants at the silica/water interface of nanoparticles is rather appealing task from the viewpoints of both fundamental and practical significance. In particular the silica surface decoration is a required step for bioanalytical application of nanoparticles [27,28], while the adsorption and further aggregation of surfactants at the silica/water interface is rather convenient alternative to covalent anchoring due to the lack of multistep purification procedures [29–32]. The previously reported silica coated Tb(III) complexes with p-sulfonatothiacalix[4]arene (42 ± 5 nm) are used as nanoparticles with lanthanide centered luminescence [33]. Luminescent Tb(III) complexes with p-sulfonatothiacalix[4]arene were used as dopants to silica nanoparticles [34]. This type of luminescent SNs can be attributed to the so-called "expanded core–shell" morphology, where luminophores are distributed both within a core and a shell, though this distribution is not homogeneous

* Corresponding author.
E-mail address: asiyamust@mail.ru (A.R. Mustafina).

0927-7765/$ – see front matter © 2011 Elsevier B.V. All rights reserved.
doi:10.1016/j.colsurfb.2011.12.015

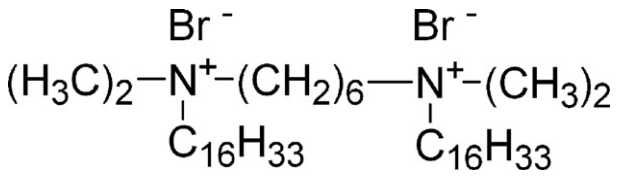

Scheme 1. Hexalidene-bis(dimethylhexadecylammonium) bromide (16-6-16).

[6]. This type of morphology is a prerequisite for the energy transfer from the silica coated donors (Tb(III) complexes) to acceptors (quenchers) at the silica/water interface. The hexalidene-bis(dimethylhexadecyl-ammonium) bromide [35,36] (16-6-16, Scheme 1) and cetyltrimethylammonium bromide (CTAB), sodium dodecylsulfate (SDS) and phospholipid (DSPG – 1,2-distearoyl-sn-glycero-3-phospho-rac-(1-glycerol) sodium salt) are chosen as surfactants, interfacially interacting with Tb-doped silica nanoparticles. The sensing is based on the quenching effect of the sulfonaphthalein dyes, namely phenol red (PhR) and bromothymol blue (BThB) on the Tb(III) centered luminescence, which is revealed from the steady state and time resolved quenching measurements. The DLS and electrokinetic potential data have been used to verify the adsorption and aggregation of surfactants at the silica surface.

2. Materials and methods

Tetraethyl orthosilicate (TEOS) 98%, ammonium hydroxide (28–30%), n-heptanol 98%, cyclohexane 99%, from Acros; terbium(III) nitrate hexahydrate (99.9%) from Alfa Aesar, Triton X-100, cetyltrimethylammonium bromide (CTAB), sodium dodecylsulfate (SDS), bromothymol blue, phenol red and 1,2-distearoyl-sn-glycero-3-phospho-rac-(1-glycerol) sodium salt from Sigma–Aldrich were used as purchased without further purification.

Hexalidene-bis(dimethylhexadecylammonium) bromide 16-6-16 (Scheme 1) was synthesized in analogy with the procedure [35,36].

Synthesis of silica coated Tb(III) nanoparticles (42 ± 5 nm) was performed according to reverse microemulsion procedure presented in the work [33].

The *dynamic light scattering* (DLS) measurements were performed by means of the Malvern Mastersize 2000 particle analyzer. A He–Ne laser operating at 633 nm wavelength and emitting vertically polarized light was used as a light source. The measured autocorrelation functions were analyzed by Malvern DTS software and the second-order cumulant expansion methods. The effective hydrodynamic radius (RH) was calculated by the Einstein–Stokes relation from the first cumulant: $D = kBT/6\pi\eta RH$, where D is the diffusion coefficient, kB is the Boltzmann constant, T is the absolute temperature, and η is the viscosity. The diffusion coefficient was measured at least three times for each sample. The average error in these experiments was approximately 4%. All samples were prepared from the bidistilled water with prior filtering through the PVDF membrane using the Syringe Filter (0.45 μm). Zeta potential "Nano-ZS" (MALVERN) using laser Doppler velocimetry and phase analysis light scattering was used for *zeta potential measurements*.

The *steady-state emission spectra* were recorded on a spectrofluorometer FL3-221-NIR (Jobin Yvon) under excitation at 330 nm.

Luminescence decay measurements were performed using a Horiba Jobin Yvon Fluorolog-3-221 spectrofluorometer with SPEX FL-1042 phosphorimeter accessory using a xenon flash lamp as the photon source with following parameters: time per flash—50.00 ms, flash count—200 ms, initial delay—0.05 ms and sample window—2 ms. Excitation of samples was performed at 330 nm, and emission detected at 546 nm with 5 nm slit width for both excitation and emission.

UV–vis spectra were recorded on a Lambda 35 spectrophotometer (Perkin-Elmer).

Surface tension measurements were performed using the du Nouy ring detachment methods.

All samples with nanoparticles were ultrasonicated within 30 min before measurements. All measurements have been performed at least three times. The pH 9.2 has been adjusted by Tris (2.5 mM).

3. Results and discussion

3.1. Decoration of SNs by cationic surfactants

The aggregation of cationic surfactants onto silica nanoparticles (SNs) is exemplified in literature in most details by CTAB [31,32].

According to these data the adsorption of cationic surfactant at a silica/water interface is revealed from the recharging of the silica surface (ζ-potential changes from minus to plus). The measurements of electrokinetic potentials reveal the recharging of Tb-doped SNs in aqueous solutions of CTAB and 16-6-16 (Fig. 1a). According to DLS measurements (Table 1) Tb-doped SNs are characterized by 200 nm aggregates in aqueous buffer solutions (Tris, 2.5 mM) at pH 9.2. The deviations between the sizes revealed from TEM (42 nm) and DLS (Table 1) greatly exceed those arisen from the

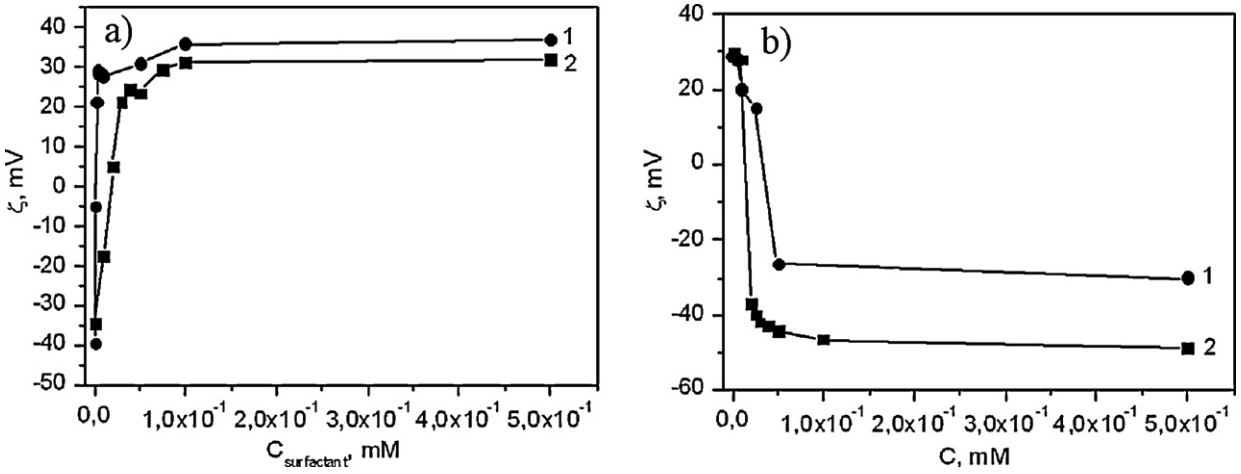

Fig. 1. The ζ-potential values (SD = 5 mV, $n = 3$) of Tb(III) doped silica nanoparticles ($C = 0.028$ g L^{-1}) versus concentration of (a): 16-6-16 (1) and CTAB (2), (b): SDS (1) and DSPG (2) at constant concentration of 16-6-16 (0.05 mM) in aqueous solutions at pH 9.2.

Table 1
Averaged hydrodynamic diameter (d) and ($n = 3$) and zeta potential (ζ) (SD = 5 mV, $n = 3$) of Tb-doped silica nanoparticles ($C = 0.028\ g\ L^{-1}$) at various concentrations of CTAB and 16-6-16, SDS and DSPG at constant concentration of 16-6-16 (5×10^{-2} mM) at pH = 9.2.

	$C_{surfactant}$, mM	d, nm	PDI	Peak means[a], nm	ζ, mV
	0	209 ± 0.55	0.186	–	−33
CTAB	0.001	220 ± 3	0.185	–	−34
	0.01	182 ± 6	0.191	–	−21
	0.02	–	0.988	127 ± 7 (28%), 1402 ± 65 (72%)	5
	0.03	–	0.595	80 ± 8 (9%), 1610 ± 42 (91%)	21
	0.04	242 ± 3	0.215	–	24
	0.05	207 ± 0.91	0.199	–	24
	0.5	205 ± 1	0.112	–	34
	1	218 ± 2	0.079	–	37
	5	206 ± 1	0.154	–	50
	10	209 ± 4	0.169	–	53
16-6-16	0.001	288 ± 1	0.209	–	−39
	0.002	–	0.705	122 ± 2 (13%), 1616 ± 107 (87%)	−5
	0.003	–	0.327	329 ± 43 (26%), 1113 ± 172 (74%)	22
	0.004	277 ± 3	0.245	–	29
	0.005	206 ± 3	0.158	–	28
	0.05	204 ± 1	0.129	–	31
	0.1	206 ± 4	0.189	–	36
	1	205 ± 1	0.156	–	49
	10	200 ± 0.80	0.171	–	53
16-6-16 + SDS	0.001	266 ± 3	0.252	–	22
	0.005	–	0.501	131 ± 41 (38%), 946 ± 254 (62%)	21
	0.01	923 ± 54	0.217	–	−13
	0.025	–	0.700	156 ± 21 (16%), 974 ± 192 (84%)	−31
	0.05	121 ± 3	0.182	–	−31
	0.5	–	0.632	117 ± 18 (21%), 521 ± 130 (69%)	−33
16-6-16 + DSPG	0.005	299 ± 8	0.282		29
	0.01	222 ± 0.20	0.288		28
	0.05	–	0.435	56 ± 2 (14%), 316 ± 0.35 (86%)	−44
	0.1	–	0.493	73 ± 19 (28%), 385 ± 57 (72%)	−47
	0.5	–	0.423	75 ± 17 (60%), 381 ± 96 (40%)	−49

[a] – at PDI > 0.300.

different working function of the two instruments, which indicates the aggregation of SNs in the these conditions. Our previous report [37] reveals the interparticle hydrogen binding and the counter ion effect of Tris buffer as main reasons of the SNs aggregation in aqueous buffer solutions. The aggregation behavior of SNs in aqueous solutions of cationic surfactants follows the ζ-potential values, being rather enhanced when ζ-potential is close to zero and coming to smaller averaged hydrodynamic diameters with the increase of ζ-potential (Table 1, Fig. 1a). Though both cationic surfactants follow this trend, there are some differences between them. In particular ζ-values of silica nanoparticles change from −33 mV in pure water to +30 mV in solution of 16-6-16 (5×10^{-3} mM), while higher concentration of CTAB (about 5×10^{-2} mM) is required for the similar recharging (Fig. 1a). The CMC for CTAB is 8.5×10^{-1} mM [38], while the CMC of 16-6-16 determined by tensiometry equals to 2×10^{-2} mM (Fig. 1S in Suppl. Data), which agrees well with literature data [39,40]. Thus the recharging of nanoparticles in solutions of cationic surfactants occurs in more diluted conditions than the aggregation of these surfactants in aqueous solutions. These results are in good agreement with the well known tendency that silica surface favors the aggregation of cationic surfactants [41–44].

3.2. Fluorescent response on the decoration of SNs with cationic surfactants

The steady state emission spectrum of Tb-doped silica nanoparticles possesses four bands peculiar for Tb-centered luminescence with the main band at 541 nm assigned to the $^5D_4$–$^7F_5$ transition [14,15]. The quenching effect of dyes on lanthanide centered luminescence is well known [45,46] and applied in bioanalysis [47] or pH measurements [48]. The quenching measurements are commonly applied to reveal molecular interactions, since the

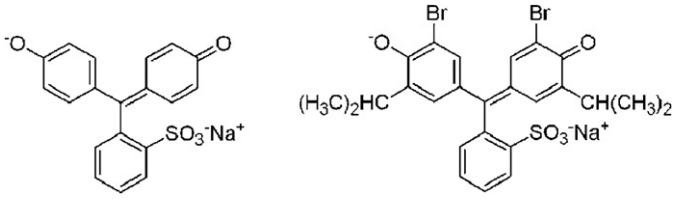

Scheme 2. Schematic representation of deprotonated forms of PhR and BThB.

quenching through the energy transfer mechanism requires the contact between fluorophore and quencher [24,25,45,46]. Thus quenching molecules should locate at the silica/water interface of nanoparticles to provide the energy transfer between the silica coated luminophores and quenching molecules. Phenol red (PhR) and bromothymol blue (BThB) (Scheme 2) which are well known sulfonaphthalein dyes have been chosen as quenching molecules. The acid/base equilibriums of both dyes exhibit detectable shift in solutions of surfactants or lipids [49–52], which is the reason of their wide application as probes of micellization [53–57] and spectral measurements of pH [58]. The pKa values are about 8.0 for PhR and 7.2 for BThB in aqueous solutions [59]. The micellization of cationic surfactants decreases the apparent pKa of both dyes due to the predominant penetration of the anionic form of dyes into cationic aggregates, which is evident from the well known spectral changes [53–59]. It is worth noting that though the acid/base equilibrium shift of PhR is sensitive to the aggregation of cationic surfactants, it cannot distinguish the aggregation occurring in the bulk of solution and at the silica/water interface of nanoparticles [31]. The pH 9.2 has been chosen for quenching measurements to exclude the shift of the acid/base equilibrium of dyes by cationic surfactants. Indeed, no detectable changes

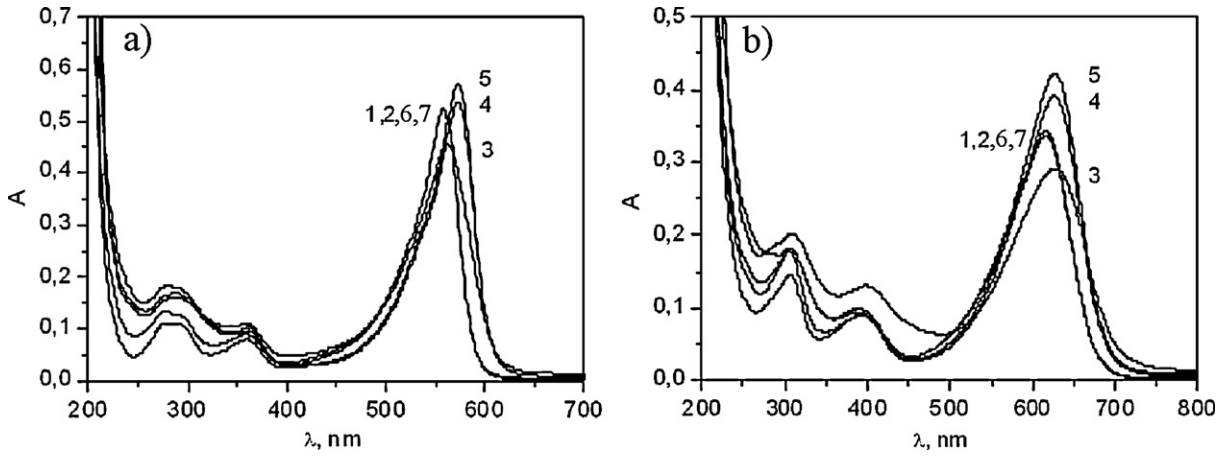

Fig. 2. The absorption spectra of PhR (a) and BThB (b) at 0.01 mM (1), in the presence of Tb-doped SNs (0.028 g L^{-1}) (2), at various amounts of 16-6-16: 0.01 mM (3); 0.05 mM (4); 0.1 mM (5); in addition of 0.5 mM of SDS (6) and DSPG (7) (at 0.05 mM of 16-6-16) at pH 9.2.

in UV–vis spectra of PhR and BThB are observed at the variation of surfactant concentrations (Fig. 2). The steady state and time resolved fluorescence measurements of Tb-doped SNs at various amounts of PhR and BThB are represented in Fig. 3 in Stern–Volmer coordinates (I_0/I versus C_{dye}, where I_0 and I are intensities of the main band at 541 nm). The fluorescence decay of Tb-doped SNs is represented in Fig. 2S (Suppl. Data), the average lifetime values used for Stern–Volmer analysis are represented in Tables 1S, 2S (Suppl. Data). Though the intensity of steady state luminescence exhibits significant decrease, which is more significant for PhR than for BThB, no significant changes of lifetimes are observed within the studied range of PhR and BThB concentrations (Fig. 3). This fact indicates that the quenching through a collision between luminescent and quenching species is not enough efficient at the concentration conditions represented in Fig. 3. Taking into account the absorbance of both dyes at 541 nm (Fig. 2) the inner filter effect of the dye being more enhanced for PhR than for BThB is responsible for the diminished intensity of steady state luminescence, while no dynamic quenching is observed in this case. It is rather anticipated that the aggregation of surfactants near the silica surface followed by the insertion of dye anions into cationic aggregates can induce the dynamic quenching. Thus the fluorescence measurements at constant concentration of the

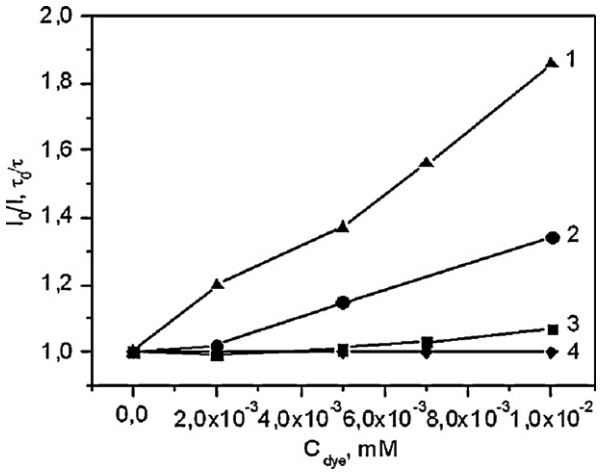

Fig. 3. The intensity based (1,2) (SD = 0.098, $n = 3$) and lifetime based (3,4) (SD = 0.02 ms, $n = 3$) Stern–Volmer plots at various concentrations of PhR (1,3) and BThB (2,4).

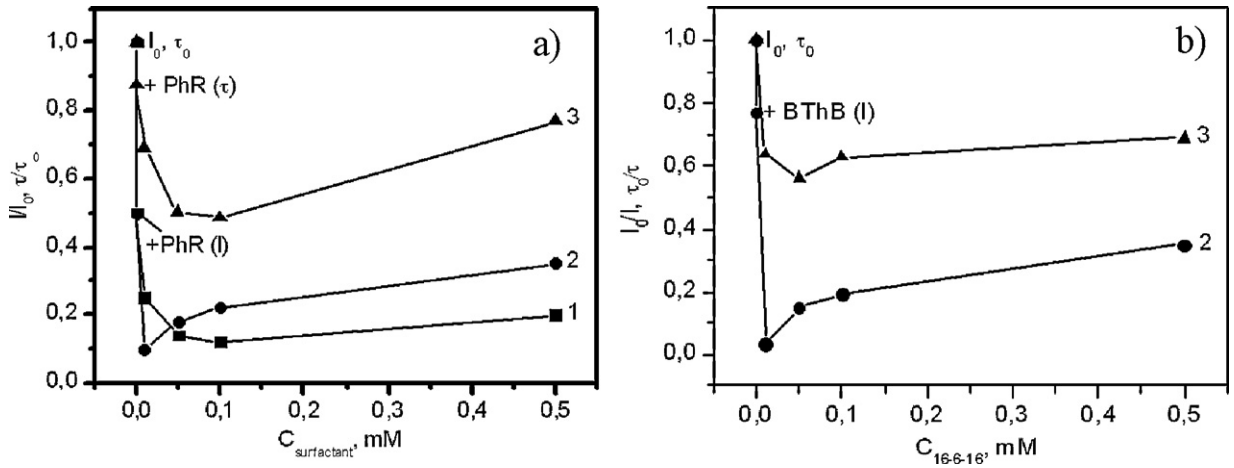

Fig. 4. The I/I_0 (SD = 0.098, $n = 3$) at various concentration of CTAB (1) and 16-6-16 (2); τ/τ_0 (SD = 0.02 ms, $n = 3$) at various concentration of 16-6-16 (3) in aqueous dispersion of SNs (0.028 g L^{-1}) in the presence of 10^{-2} mM of PhR (a) and BThB (b) at pH 9.2; I_0 is the emission intensity without dyes. The I/I_0 and τ/τ_0 values without surfactants are designated as "+PhR (I)", "+BThB (I)" and "+PhR (τ)" correspondingly.

quencher (0.01 mM) and various concentrations of 16-6-16 and CTAB have been performed with the aim to reveal the quenching effect versus surfactant aggregation near Tb-doped SNs. The choice of the quencher concentration is determined by two reasons. The concentration of the dye should be enough to provide significant energy transfer between silica coated Tb(III) complexes and dye anions at definite concentration of cationic surfactant, while the inner filter effect of the latter should be restricted. To simplify the quenching regularities the emission intensity (I) has been converted to a relative form (I/I_0), which indicates the extent of quenching. Fig. 4a represents I/I_0 versus surfactant concentration at 0.01 mM of PhR. The obtained results indicate the most enhanced quenching at 10^{-2} mM of 16-6-16 and 10^{-1} mM of CTAB. The partial reestablishment of the Tb(III)-centered luminescence of SNs with further increase of surfactant concentration is observed for both cationic surfactants.

These quenching regularities do not agree with the absorption intensity of PhR at 541 nm (Fig. 2), indicating that the inner filter effect of PhR is not responsible for the enhanced quenching at definite surfactant concentration. Moreover the quenching regularities are the same for PhR and BThB (Fig. 4), though these dyes exhibit different inner filter effect on the Tb-centered luminescence of SNs (Fig. 2). Thus time resolved luminescence measurements have been performed at various concentrations of 16-6-16 in the presence of both dyes (Tables 1S, 2S in Suppl. Data). The decrease of τ/τ_0 at 10^{-2} mM of 16-6-16 reveals significant dynamic quenching, while further increase of surfactant concentration results in the reestablishment of lifetimes. The comparative analysis of I/I_0 (τ/τ_0) and ξ-values at various surfactant concentrations reveals good correlation between the quenching through the energy transfer and recharging of SNs (Figs. 1 and 4). Thus the energy transfer between luminophores within silica nanoparticles (donors) and dye anions (acceptors) is favored when dye anions penetrate into surfactant aggregates near the silica surface. It is worth noting that the quenching effect gradually comes to the initial level (I/I_0 without surfactant) at the surfactant concentration higher than 10^{-2} mM of 16-6-16 and 10^{-1} mM of CTAB. Taking into account that the micellization predominantly occurs in the bulk of solution at higher surfactant concentrations, the penetration of dye anions into the aggregates, which are far from the

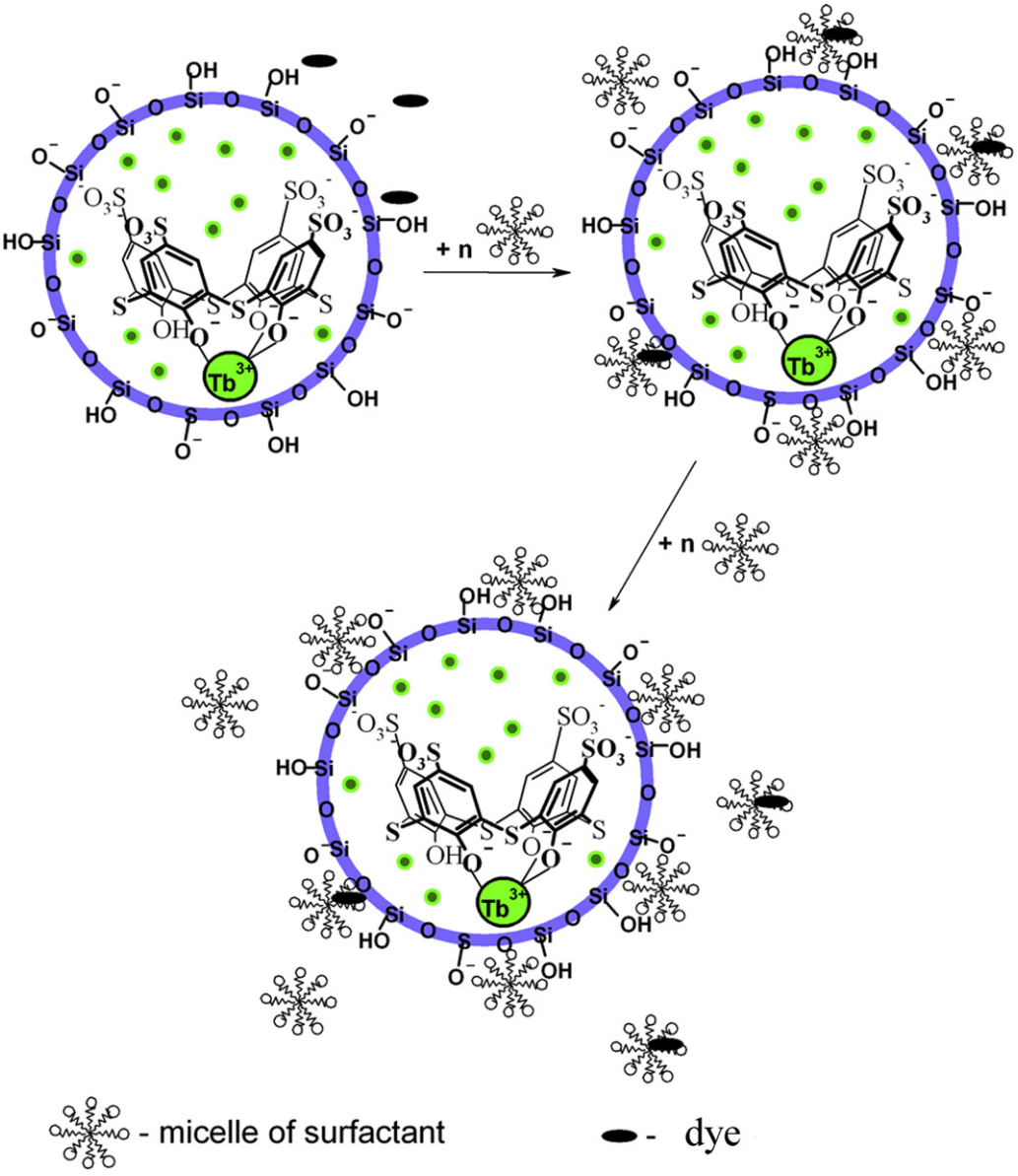

Scheme 3. Schematic representation of the penetration of dye anions into surfactant aggregates at the silica/water interface and in the bulk of solution.

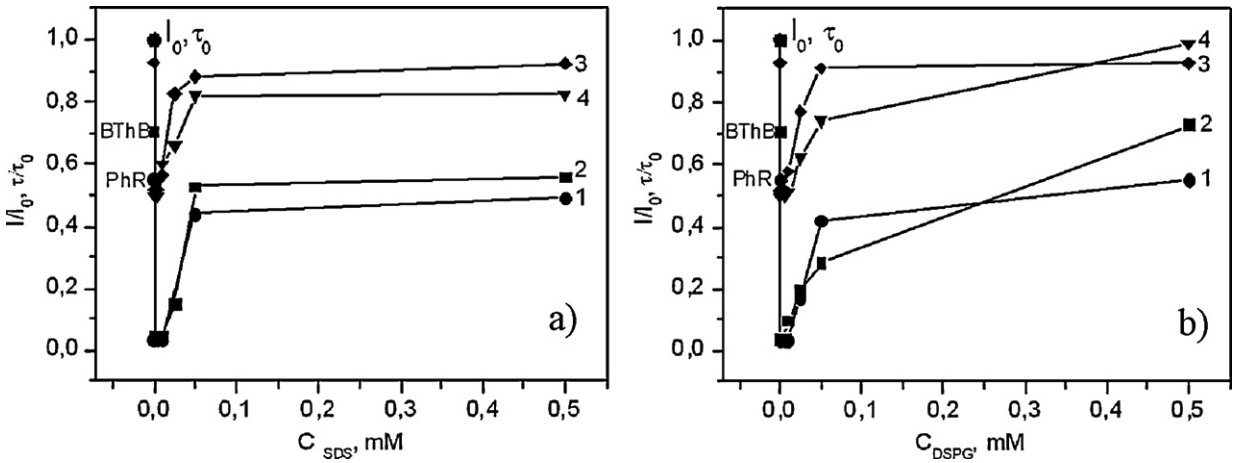

Fig. 5. The I/I_0 (1,2) (SD = 0.098, $n = 3$) and τ/τ_0 (3,4) (SD = 0.02 ms, $n = 3$) at various concentrations of SDS (a) and DSPG (b) in aqueous dispersion of SNs (0.028 g L^{-1}) pretreated by 16-6-16 (0.01 mM) in the presence of 10^{-2} mM of PhR (1,3) and BThB (2,4) at pH 9.2; I_0 and τ_0 are the emission intensity and lifetime without dyes. The I/I_0 values without surfactants are designated as "PhR" and "BThB".

silica surface explains the reestablishment of the Tb-centered luminescence (Scheme 3). It is worth noting that the quenching effect at various surfactant concentrations distinguishes the aggregation of cationic surfactants near the silica nanoparticles and in the bulk of solution.

Both the aggregation of surfactants onto silica and the insertion of dye anions into these aggregates should be mentioned as the key factors responsible for the quenching through the energy transfer between dye anions and Tb complexes within silica nanoparticles.

3.3. The recognition of SDS and DSPG with the use of Tb-doped SNs

It is obvious that electrostatic attraction together with Van der Waals interactions predominantly contribute to the binding of dye anions with cationic aggregates. Thus the displacement of dye anions from cationic aggregates at the silica/water interface can result from the competitive interactions with another amphiphilic anions. The choice of sodium dodecylsulfate (SDS) and DSPG as amphiphilic anions derives from their high affinity to cationic aggregates, resulting in the mixed anionic–cationic surfactant aggregation [60–64]. Indeed, the addition of sodium dodecylsulfate (SDS), as well as DSPG to Tb-doped SNs in solution of 16-6-16 (0.01 mM) results in the mixed aggregation, which occurs in the bulk of solution and at the interface of SNs (Fig. 1b). The mixed aggregation in the bulk of solution is evident from the appearance of mixed aggregates (Table 1), while the latter process is evident from the recharging of SNs, which is more enhanced for DSPG in the comparison with SDS (Fig. 1b). The DLS data indicate that the aggregation behavior of nanoparticles follows their electrokinetic potential values (Fig. 1b, Table 1). The analysis of ξ-values and DLS data reveals the difference in the mixed aggregation of SDS and DSPG with 16-6-16 both in the bulk of solution and at the silica/water interface of SNs (Fig. 1b, Table 1), which is in good agreement with CMC of SDS and DSPG [65,66]. Thus the quenching effect of both dyes has been analyzed in binary anionic–cationic surfactant solutions at various concentrations of anionic amphiphiles and 0.01 mM of 16-6-16.

Fig. 5 represents the I/I_0 of Tb-centered luminescence of SNs at constant concentration of both dyes (0.01 mM) in aqueous solution (as a single points I_{BTB} and I_{PhR}) and in solution of 16-6-16 (0.01 mM) at various concentrations of SDS and DSPG. Indeed, the addition of SDS and DSPG to Tb-doped SNs at 0.01 mM of 16-6-16 "switches on" Tb-centered luminescence. The concentrations of SDS and DSPG, where "switching on" occurs, agree well with the recharging of SNs from plus to minus (Figs. 5 and 1b). Thus the reasons of the "switching on" are worth discussing. As it has been above mentioned the I/I_0-value of SNs at 0.01 mM of the dye is conditioned by the inner filter effect without any contribution of the quenching through dynamic mechanism. The inner filter effect of dyes stays practically unchanged with the variation of DSPG and SDS concentrations at 0.01 mM of 16-6-16 (Fig. 2). Thus the increase of I/I_0-value with the growth of SDS and DSPG concentrations reflects the decreased contribution of the quenching through dynamic mechanism due to the displacement of dye anions by amphiphilic anions, which is confirmed by time resolved luminescence measurements (Fig. 5, Tables 1S, 2S in Suppl. Data). Though the increase of luminescence intensity is observed for SDS, DSPG and both dyes, some differences between them indicate that the structure of both substituting and replaceable anions affects the displacement of dyes by amphiphilic anions at the interface of silica coated Tb complexes. Thus both the efficiency of the displacement and "off–on" switching of luminescence may be sensitive to the structure of substituting anions. This assumption should be confirmed by further studies, which we are going to perform in the nearest future.

4. Conclusions

Summarizing the obtained results following points are worth noting:

The obtained results represent the energy transfer from the silica coated Tb(III) complexes to phenol red and bromothymol blue dyes at the interface of silica nanoparticles as a route to probe into the aggregation of surfactants at the silica/water interface. The interfacial binding of dye anions with SNs in aqueous solutions is insignificant due to the negatively charged silica surface. Thus no dynamic quenching is revealed at these conditions. The adsorption and further aggregation of cationic surfactants at the silica/water interface of Tb-doped SNs greatly favors their interfacial interactions with dye anions, which is followed by the enhanced quenching effect of dyes on Tb centered luminescence. The latter originates from the donor–acceptor energy transfer between silica coated Tb complexes and dye anions at the silica/water interface. Thus both the steady state and time resolved quenching measurements enable to reveal the concentration conditions of predominant aggregation of cationic surfactants near the silica surface, which are peculiar for various surfactants exemplified by

CTAB and 16-6-16. The mixed cationic–anionic aggregation near the silica surface exemplified for 16-6-16-SDS (DSPG) results in the "off–on" switching of Tb-centered luminescence. The obtained "on–off–on" switching of Tb-centered luminescence correlates with the "minus–plus–minus" recharging of the silica surface. The latter is verified by the ξ-potential measurements. So, the present work introduces the interactions of dye anions with silica surface as a simple route to reveal the aggregation of surfactants and phospholipids at the interface of the lanthanide doped SNs. The obtained results represent novel approach to make substrate responsive colloids from lanthanide doped SNs, which in turn should widen their applicability in biosensing.

Acknowledgement

We thank RFBR (project N 10-03-00352-a) for financial support.

Appendix A. Supplementary data

Supplementary data associated with this article can be found, in the online version, at doi:10.1016/j.colsurfb.2011.12.015.

References

[1] D. Knopp, D. Tang, R. Niessner, Anal. Chim. Acta 647 (2009) 14.
[2] H. Wu, Q. Huo, S. Varnum, J. Wang, G. Liu, Z. Nie, J. Liu, Y. Lin, Analyst 133 (2008) 1550.
[3] W.-C. Law, K.-T. Yong, I. Roy, G. Xu, H. Ding, E. Bergey, H. Zeng, P. Prasad, J. Phys. Chem. C 112 (2008) 7972.
[4] C. Ren, J. Li, X. Chen, Z. Hu, D. Xue, Nanotechnology 18 (2007) 345604.
[5] I. Roy, T. Ohulchaskyy, D. Bharali, H. Pudavar, R. Mistretta, N. Kaur, P. Prasad, PNAS 102 (2005) 279.
[6] D. Larson, H. Ow, H. Vishwasrao, A. Heikal, U. Wiesner, W. Webb, Chem. Mater. 20 (2008) 2677.
[7] J.-Q. Gu, J. Shen, L.-D. Sun, C.-H. Yan, J. Phys. Chem. C 112 (2008) 6589.
[8] S. Pihlasalo, J. Kirjavainen, P. Hänninen, H. Härmä, Anal. Chem. 83 (2011) 1163.
[9] L. Wang, W. Zhao, W. Tan, Nano Res. 1 (2008) 99.
[10] A. de Dios, M. Díaz-García, Anal. Chim. Acta 666 (2010) 1.
[11] L. Latterini, M. Amelia, Langmuir 25 (2009) 4767.
[12] B. Trewyn, S. Giri, I. Slowing, V. Lin, Chem. Commun. 31 (2007) 3236.
[13] X. Zhou, J. Zhou, Anal. Chem. 76 (2004) 5302.
[14] S. Eliseeva, J.-C. Bünzli, Chem. Soc. Rev. 39 (2010) 189.
[15] S. Plush, T. Gunlaugsson, Dalton Trans. 29 (2008) 3801.
[16] Z. Ye, M. Tan, G. Wang, J. Yuan, Talanta 65 (2005) 206.
[17] F. Enrichi, R. Ricco, P. Scopece, A. Parma, A. Mazaheri, P. Riello, A. Benedetti, Nanopart. Res. 12 (2010) 1925.
[18] F. Gao, F. Luo, X. Chen, W. Yao, J. Yin, Zh. Yao, L. Wang, Talanta 80 (2009) 202.
[19] H. Jiang, G. Wang, W. Zhang, X. Liu, Z. Ye, D. Jin, J. Yuan, Zh. Liu, J. Fluoresc. 20 (2010) 321.
[20] K. Binnemans, P. Lenaerts, K. Driesen, Ch. Görller-Walrand, J. Mater. Chem. 14 (2004) 191.
[21] Ch. Wu, J. Hong, X. Guo, Ch. Huang, J. Lai, J. Zheng, J. Chen, X. Mu, Y. Zhao, Chem. Commun. 6 (2008) 750.
[22] H. Härmä, Ch. Graf, P. Hänninen, J. Nanopart. Res. 10 (2008) 1221.
[23] S. Pihlasalo, J. Kirjavainen, P. Hänninen, H. Härma, Anal. Chem. 83 (2011) 1163.
[24] P. Selvin, T. Rana, J. Hearst, J. Am. Chem. Soc. 116 (1994) 6029.
[25] J. Lakowicz, Principles of Fluorescence Spectroscopy. Quenching of Fluorescence, Kluwer Academic, New York, 1999.
[26] H. Härmä, L. Dähne, S. Pihlasalo, J. Suojanen, J. Peltonen, P. Hänninen, Anal. Chem. 80 (2008) 9781.
[27] L. Wang, K. Wang, S. Santra, X. Zhao, L. Hilliard, J. Smith, Y. Wu, W. Tan, Anal. Chem. 78 (2006) 646.
[28] G. Orts-Gil, K. Natte, D. Drescher, H. Bresch, A. Mantion, J. Kneipp, W. Osterle, J. Nanopart. Res. 13 (2011) 1593.
[29] H. Wei, J. Liu, L. Zhou, J. Li, X. Jiang, J. Kang, X. Yang, S. Dong, E. Wang, Chem. A: Eur. J. 14 (2008) 3687.
[30] H. Mori, A. Muller, J. Klee, J. Am. Chem. Soc. 125 (2003) 3712.
[31] E. Bryleva, N. Vodolazkaya, N. Mchedlov-Petrossyan, L. Samokhina, N. Matveevskaya, A. Tolmachev, J. Colloid Interface Sci. 316 (2007) 712.
[32] W. Wang, B. Gu, L. Liang, W. Hamilton, J. Phys. Chem. B 108 (2004) 17477.
[33] A. Mustafina, S. Fedorenko, O. Konovalova, A. Menshikova, N. Shevchenko, S. Soloveva, A. Konovalov, I. Antipin, Langmuir 25 (2009) 3146.
[34] A. Mirgorodskaya, L. Kudryavtseva, V. Pankratov, S. Lukashenko, L. Rizvanova, A. Konovalov, J. Gen. Chem. 76 (2006) 1696.
[35] N. Iki, T. Horiuchi, K. Koyama, N. Morohashi, Ch. Kabuto, S. Miyano, J. Chem. Soc., Perkin Trans. 2 (2001) 2219.
[36] N. Iki, T. Fujimoto, S. Miyano, Chem. Lett. 27 (1998) 625.
[37] A.R. Mustafina, J.G. Elistratova, O.D. Bochkova, V.A. Burilov, S.V. Fedorenko, A.I. Konovalov, S. Ye Soloveva, J. Colloid. Interface Sci. 354 (2011) 644.
[38] L. Zakharova, F. Valeeva, A. Zakharov, A. Ibragimova, L. Kudryavtseva, H. Harlampidi, J. Colloid Interface Sci. 263 (2003) 597.
[39] R. Zana, M. Benrraou, R. Rueff, Langmuir 7 (1991) 1072.
[40] Kabir-ud-Din, W. Fatma, S. Khatoon, Z. Khan, A. Naqvi, J. Chem. Eng. Data 53 (2008) 2291.
[41] C. Chorro, M. Chorro, O. Dolladile, S. Partyka, R. Zana, J. Colloid. Interface Sci. 199 (1998) 169.
[42] S. Parida, S. Dash, S. Patel, B. Mishra, Adv. Colloid Interface Sci. 121 (2006) 77.
[43] R. Lamont, W. Ducker, J. Am. Chem. Soc. 120 (1998) 7062.
[44] J.-F. Liu, W. Ducker, J. Phys. Chem. B 103 (1999) 8558.
[45] R. Srour, L. McDonald, J. Chem. Eng. Data 53 (2008) 116.
[46] S. Lis, M. Elbanowski, B. Makowska, Z. Hnatejko, J. Photochem. Photobiol. A: Chem. 150 (2002) 233.
[47] T. Wensel, C. Meares, J. Less Common Met. 149 (1989) 143.
[48] M. Kessler, Anal. Chem. 71 (1999) 1540.
[49] N. Mchedlov-Petrossyan, Pure Appl. Chem. 80 (2008) 1459.
[50] R. Kumar, D. Milanova, Ann. N. Y. Acad. Sci. 1161 (2009) 472.
[51] J. Rimer, R. Lobo, D. Vlachos, Langmuir 21 (2005) 8960.
[52] B. Boruah, P. Saikia, B. Gohain, R. Dutta, J. Mol. Liq. 151 (2010) 81.
[53] N. Mchedlov-Petrossyan, N. Vodolazkaya, Y. Gurina, W.-C. Sun, K. Gee, J. Phys. Chem. B 114 (2010) 4551.
[54] P. Levitz, H. Van Damme, D. Keravis, J. Phys. Chem. 88 (1984) 2228.
[55] P. Levitz, H. Van Damme, J. Phys. Chem. 90 (1986) 1302.
[56] N. Turro, A. Yekta, JACS 100 (1978) 5951.
[57] S. Manne, G. Warr, Supramolecular structure in confined geometries, in: Supramolecular Structure of Surfactants Confined to Interfaces, ACS, Washington, DC, 1999 (Chapter 1).
[58] L. Hench, I. West, Chem. Rev. 90 (1990) 33.
[59] E. Bishop, Indicators, vol. 1, Pergamon Press, Oxford, 1972.
[60] V. Tomasic, I. Stefanic, N. Filipovic-Vincekovic, Colloid Polym. Sci. 277 (1999) 153.
[61] R. Nagarajan, Adv. Colloid Interface Sci. 26 (1986) 205.
[62] J. Hao, H. Hoffmann, Curr. Opin. Colloid Interface Sci. 9 (2004) 279.
[63] D.-Zh. Sun, X.-L. Wei, B.-L. Yin, Sh-B. Wang, Thermochim. Acta 407 (2003) 11.
[64] M. Haque, A. Das, A. Rakshit, S. Moulik, Langmuir 12 (1996) 4084.
[65] M. Bakshi, P. Kohli, Indian J. Chem. 36A (1997) 1075.
[66] E. Dennis, Adv. Colloid Interface Sci. 26 (1986) 55.